ADVANCED MATERIALS
www.advmat.de

Wetting-Transparent Graphene Films for Hydrophobic Water-Harvesting Surfaces

Gun-Tae Kim, Su-Ji Gim, Seung-Min Cho, Nikhil Koratkar, and Il-Kwon Oh**

Our current understanding of wetting of graphene-coated surfaces is that graphene is wetting-transparent provided that the underlying surface is significantly more wettable than graphene, while it is wetting-opaque for surfaces that are less wettable than graphene.[1–8] Here we show that graphene coatings can in fact be wetting-transparent even for roughened copper surfaces which by virtue of their entrapped air-pockets are significantly less wettable than graphene itself. This contradictory result is explained by the fact that the graphene film in our case is grown 'in-situ' by chemical-vapor-deposition on the roughened copper surface. The graphene coating therefore conforms perfectly to the roughness features of the copper substrate as opposed to previous studies[1,8] with transferred graphene films that simply sat on top of the roughness features. We show that such graphene films offer excellent resistance to copper corrosion while maintaining the intrinsic hydrophobicity of the surface, enabling superior performance for water-harvesting applications.

It is important both from a fundamental standpoint and for practical applications to understand how water wets free-standing graphene and graphene-coated surfaces. Several studies[1–3] have used molecular dynamics to predict the intrinsic water contact angle of a monolayer (free-standing) graphene sheet that is isolated from substrate effects. These studies predict a water contact angle of graphene between 96° and 102° which is much larger than the contact angle of bulk graphite (~90°). It should be noted here that a recent study[4] showed that these estimates include the effect of a monolayer of hydrocarbon contamination that typically forms on graphitic surfaces. Without the hydrocarbon layer, graphite and graphene are shown to be hydrophilic[4] and not hydrophobic as is generally accepted. However given that such hydrocarbon contamination is unavoidable in practical applications, let us consider the graphite water contact angle to be ~90° and the isolated graphene water contact angle to be ~100°. When graphene is used to coat a surface that interacts with water predominantly via non-bonding (*i.e.* van der Waals) interactions, the graphene coating is shown to be wetting-transparent[5,6] provided that the surface being coated is significantly more wettable than graphene itself. This is an artifact of the extreme thinness[5,7] of graphene which enables partial transmission[1,2] of the van der Waals interactions between water and the underlying substrate. However the situation is reversed when the surface that is being coated is more hydrophobic than graphene. For example, in Ref. [1] and Ref. [8] nanostructured (rough) surfaces with water contact angle of >120° were used as the substrate onto which monolayer graphene was transferred by wet chemical transfer techniques. Both these studies indicated that the water contact angle of the graphene coated surface is now dominated by the graphene coating and is ~100° as would be expected for an isolated graphene sheet.[1–3] In such a situation, the graphene coating is in fact wetting-opaque[1,8] and not wetting-transparent.

Hydrophobic (rough) surfaces with entrapped air pockets have many important technological applications which include water harvesting, anti-fouling, self-cleaning, low-friction and drag coatings as well as in two-phase heat transfer processes such as condensation and pool-boiling.[9–12] Coating such surfaces with graphene could potentially enhance the corrosion/oxidation resistance and chemical stability of such surfaces. However the aforementioned 'wetting opacity' of graphene on such textured (rough) surfaces significantly reduces the hydrophobicity of the surface and is therefore a major drawback for practical applications. Here we show that contrary to conventional wisdom, graphene can indeed preserve the hydrophobicity of textured surfaces when it is grown 'in-situ' by chemical deposition methods as opposed to being transferred onto the rough surfaces by wet chemistry based approaches.[8,13] We show that such wetting-transparent graphene films impart excellent corrosion resistance and chemical stability to the surface. We also demonstrate an important practical application of such a surface for harvesting water from the environment via dehumidification.

Scheme 1 shows a schematic diagram of our fabrication method. To make the copper surface hydrophobic, it is necessary to roughen it so as to generate entrapped air pockets. The

G.-T. Kim, Prof. I.-K. Oh
Graphene Research Center
KAIST Institute for the Nano Century
School of Mechanical
Aerospace and Systems Engineering
Division of Ocean Systems Engineering
Korea Advanced Institute of Science
and Technology (KAIST)
335 Gwahak-ro, Yuseong-gu, Daejeon 305–701, Republic of Korea
E-mail: ikoh@kaist.ac.kr
S.-J. Gim
School of Chemical and Biomolecular Engineering
Korea Advanced Institute of Science and Technology (KAIST)
335 Gwahak-ro, Yuseong-gu, Daejeon 305–701, Republic of Korea
S.-M. Cho
Micro Device & Machinery Solution Division
SAMSUNG Techwin R&D Center
Seongnam-si, Gyeonggi-do 463–400, Republic of Korea
N. Koratkar
Department of Materials Science and Engineering and the
Department of Mechanical
Aerospace, and Nuclear Engineering
Rensselaer Polytechnic Institute
110 8th Street, Troy, New York 12180, USA
E-mail: koratn@rpi.edu

DOI: 10.1002/adma.201401149

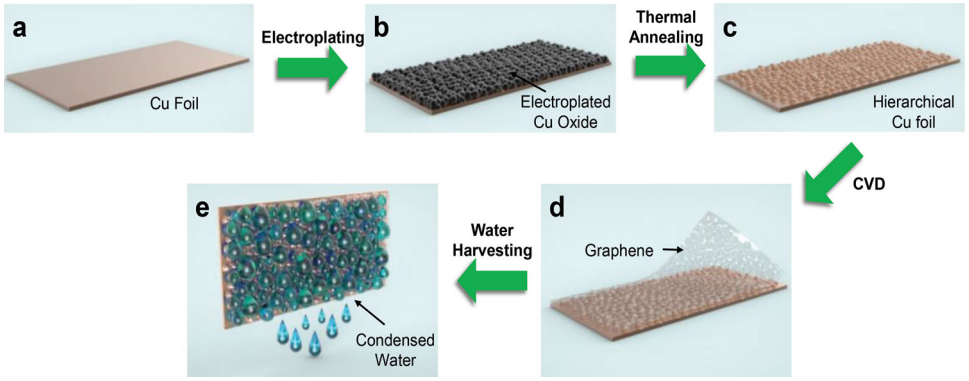

Scheme 1. Schematic of monolayer graphene coating on a hydrophobic electroplated copper surface. (a) Flat copper substrate, (b) Hierarchical roughened structure of copper oxide grown on the copper substrate by electroplating, (c) Electroplated (rough) copper substrate obtained after thermal annealing, (d) Monolayer graphene coating grown in-situ by chemical vapor deposition onto the substrate in (c), and (e) Water harvesting by the corrosion resistant (graphene protected) hydrophobic copper surface. The graphene coating is wetting-transparent and therefore does not perturb the intrinsic hydrophobicity of the underlying (rough) copper surface.

copper surface was roughened by electroplating (Figure S1) in ~0.06 M sulfuric acid (H_2SO_4) and ~0.08 M copper sulfate ($CuSO_4$) aqueous solution at ambient temperature. The electroplated copper oxide particles form hierarchical surface roughness structures on the copper foil. Next we grow graphene *in-situ* on this roughened copper surface by thermal chemical vapor deposition (CVD).[14,15] Prior to exposing the substrate to hydrocarbon gases for CVD growth, the surfaces are first thermally annealed at ~850 °C in vacuum. During thermal annealing, the electrodeposited copper oxide particles are reduced to copper particles and impurities are removed. In the final step, graphene is synthesized on the roughened copper foil by CVD using methane as the hydrocarbon source (see Experimental Section and Figures S2 and S3). It should be noted that at the high temperatures associated with annealing and subsequent CVD growth, the electroplated copper particles are vaporized far more easily than the bulk copper. Consequently it is crucial that the electroplated (rough) copper film has sufficient thickness (see Experimental Section) to withstand the annealing and CVD growth conditions.

Scanning electron microscopy (SEM) was used to characterize the surface of the copper foils. **Figures 1**a, b, c and d represent the morphology of baseline copper (designated as Cu), electroplated copper (designated as h-Cu), electroplated and thermal-annealed copper (designated as h-rCu), and electroplated and thermal annealed copper with graphene (designated as h-Gr/rCu), respectively. Photographs of sessile water drops placed on these surfaces are shown in the insets with the measured water contact angle. The morphology of the electroplated copper foil (Figure 1b) showed a dramatic increase in roughness as compared to the baseline copper foil. After thermal annealing (Figure 1c) and CVD growth of graphene (Figure 1d), the morphology of the Cu foils undergo further changes. The copper foils were heated to ~850 °C during thermal annealing and ~1000 °C during the CVD process. At these high temperatures, the electroplated copper grains on the surface were melted and vaporized. As a result, the quantity of electroplated copper particles was significantly reduced and the melted copper grains adhered to each other. In spite of this the h-rCu and h-Gr/rCu surfaces shown in Figures 1c and d are significantly rougher than the baseline copper surface (Figure 1a). In addition to graphene growth on the electrodeposited (rough) copper surface, we also performed graphene growth on the baseline (flat) copper surface to serve as a control. Raman spectroscopy characterization was used to confirm that graphene growth has taken place on the samples (see Experimental Section). The measured Raman spectra from the Gr/Cu and h-Gr/rCu samples are shown in the Figure S4; the G and 2D peaks are evident in the Raman spectra. By contrast the defect related D peak is conspicuously absent which indicates the high quality and continuous nature of the graphene coating on the copper surfaces. The ratio of the intensity of the Raman G and 2D band peaks is ~0.4 which indicates predominantly monolayer[14–16] growth of graphene on the copper foils. In addition, we also transferred the graphene films onto Si/SiO_2 substrates by wet-chemistry based methods and repeated the Raman characterization. The results (shown in Figure 1e) indicate that the intensity ratio of the G and 2D peaks is ~0.4 to 0.5 which confirms that the graphene coating is comprised of predominantly monolayer graphene.[14–16]

Water contact angle measurements using the sessile drop method (see Experimental Section) are shown in Figure 1f. Wetting measurements were performed on at least five different locations on the sample surface and then averaged for statistics. The baseline (flat) copper surface shows a water contact angle of ~86°. The contact angle remains ~86° when the baseline copper is coated (by CVD) with a monolayer graphene film (Figures S5a and b). This confirms that the graphene film is 'wetting-transparent' for a flat copper surface consistent with Ref. [5]. The electroplated copper surface (h-Cu) without graphene coating or thermal annealing is superhydrophilic with water contact angle of ~19° (Figure S5c). This is expected because the electrodeposited copper oxide particles are hydrophilic and therefore a roughened surface comprised of such hydrophilic particles is expected to display super-hydrophilic behavior consistent with the well-established Wenzel model[17,18] for wetting of rough surfaces. After thermal annealing of the electroplated copper surface, the water contact angle rises to ~128° (Figure S5d). This is also expected since the thermal annealing reduces the electrodeposited copper oxide

Adv. Mater. **2014**,
DOI: 10.1002/adma.201401149

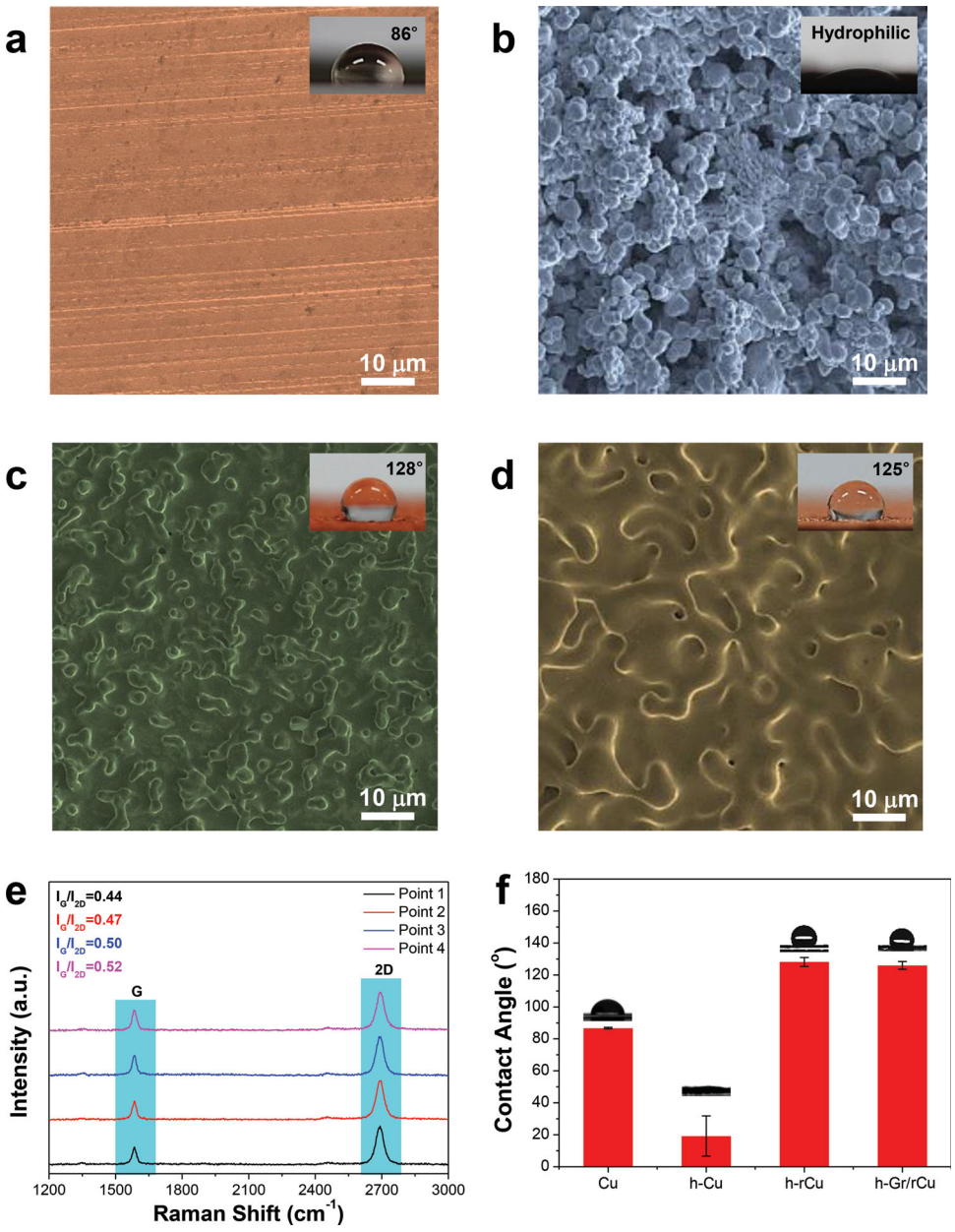

Figure 1. Surface characterization and static water repellency of the hydrophobic graphene-coated copper surface. Scanning electron microscopy (SEM) images of (a) Bare copper substrate (Cu), (b) Electroplated copper substrate (h-Cu), (c) Electroplated and thermal annealed copper substrate (h-rCu), (d) Electroplated and thermal annealed copper after graphene growth (h-Gr/rCu) by chemical vapor deposition. The insets show photographs of water droplets on each surface. (e) Raman spectra of graphene coating after transfer to a SiO_2/Si substrate. (f) Static water contact angle measurements on the Cu, h-Cu, h-rCu and h-Gr/rCu surfaces.

particles to copper. Since copper has a relatively high water contact angle of ~86° (Figure S5a), a roughened copper surface with entrapped air pockets will display strong water repellency consistent with the Cassie-Baxter wetting model.[18,19] However what is surprising is that after graphene growth on the electroplated and thermally-reduced copper surface, the water contact angle (~125°) remains close to the value before graphene deposition (Figure S5e). This means that the graphene coating shows wetting-transparency even though the underlying roughened copper surface (with water contact angle ~128°) is far more hydrophobic than the graphene (contact angle ~100°) itself. Previous studies in which graphene was transferred onto roughened super-hydrophobic surfaces (including roughened copper surfaces)[1,8] showed wetting-opacity which contradicts the current findings. It appears that the primary reason for this deviation is the deposition method used in this work when compared to prior studies. In prior work, graphene was first grown on copper and then transferred onto the rough surface using wet chemistry methods that utilize a sacrificial polymer transfer film.[8,13] For such cases, the graphene film remains

ADVANCED MATERIALS
www.advmat.de

www.MaterialsViews.com

relatively flat and simply sits on the top of the surface roughness features (for example, see Figure S6 for graphene transfer onto a rough copper surface). In such a scenario, the water drop encounters a flat, nearly free-standing graphene sheet that is decoupled from the underlying surface, which implies that the wetting is dictated by the graphene sheet itself leading to wetting-opacity.

In the present case, the deposition method is based on in-situ CVD growth of graphene on the roughened copper surface. Since carbon has very low solubility in copper, the mechanism of graphene growth involves surface adsorption[14,15] of carbon atoms on the copper surface. Once a monolayer of graphene is formed the process becomes self-limiting and further graphene growth is suppressed. Since the graphene growth process is based on surface adsorption, it is clear that the as-deposited graphene film will adhere and conform to the surface topology of the roughened copper surface. Consequently, in spite of the graphene coating, the water drop continues to experience the surface porosity (with entrapped air pockets) that renders it strongly water repellent. These results indicate that it is indeed possible to retain the strong water repellency of textured (rough) surfaces by draping the surface with monolayer graphene films that are well-adhered to the surface and follow the contours of the surface. Such graphene coatings show coincidental wetting-transparency even for strongly hydrophobic (rough) surfaces with water contact angles >120°.

We evaluated the ability of the graphene drape to suppress the oxidation and corrosion of the underlying copper surface. For this, the graphene-coated copper surfaces as well as baseline (uncoated) copper surfaces were heated in a furnace for 4 h at 200 °C. **Figure 2** shows photographs and X-ray photoelectron spectroscopy (XPS) measurements of copper surfaces before and after oxidation in air. In cases of bare copper (Cu) as well as electroplated and annealed bare copper (h-rCu), the surface color is dramatically changed, but the graphene-coated copper surfaces (Gr/Cu and h-Gr/rCu) show only a slight change in color. In Gr/Cu (Figure 2b) and h-Gr/rCu (Figure 2d) samples, the XPS spectra show two sharp Cu peaks before and after thermal annealing, which correspond to Cu($2P_{1/2}$) and Cu($2P_{3/2}$), respectively.[20,21] However, Cu (Figure 2a) and h-rCu

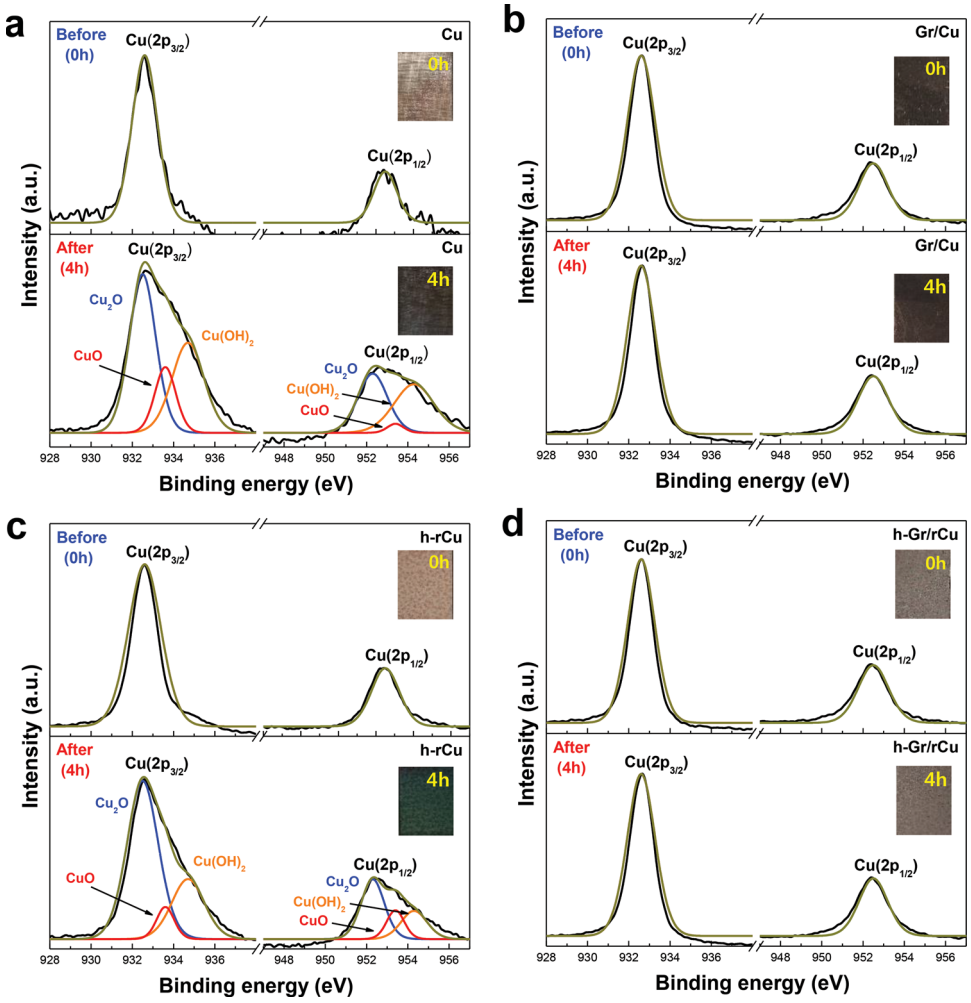

Figure 2. Oxidation resistance of graphene-coated hierarchical (hydrophobic) copper surface. XPS analysis corresponding to Cu$2p_{3/2}$ and Cu$2p_{1/2}$ spectrum of (a) flat copper, (b) Graphene-coated flat copper, (c) electroplated and thermal annealed copper without graphene coating and (d) with graphene coating before (upper) and after (lower) air annealing. The insets show photographs of each samples taken before and after thermal annealing in air (200 °C, 4 h).

Adv. Mater. **2014**,
DOI: 10.1002/adma.201401149

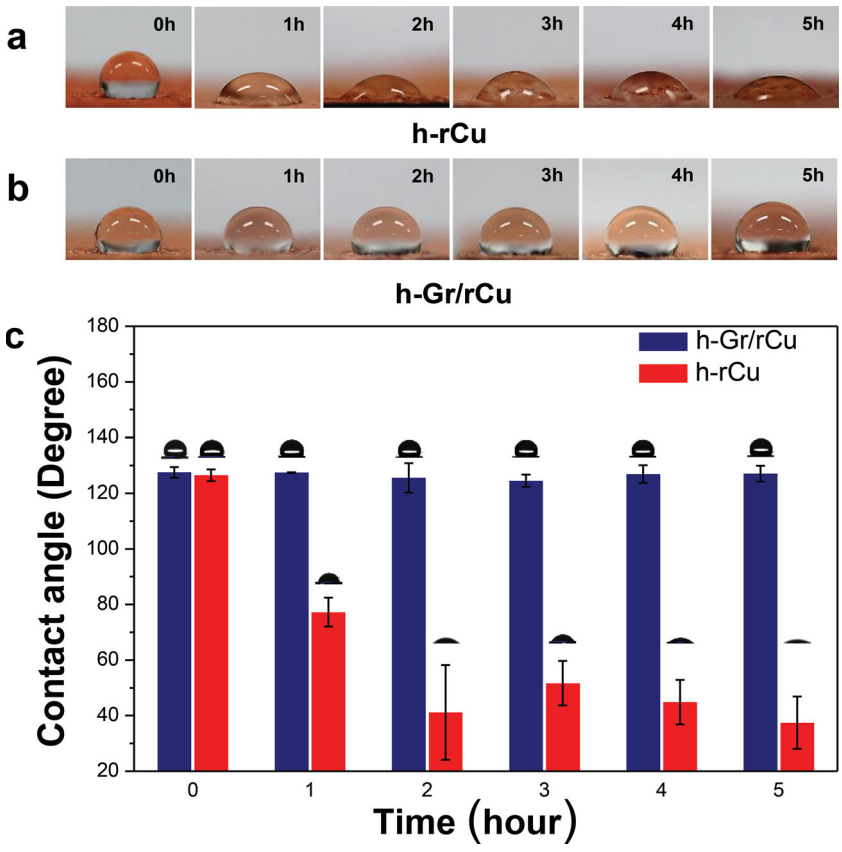

Figure 3. Chemical stability and robustness of the surface hydrophobicity. Photographs of water droplets on (a) h-rCu and (b) h-Gr/rCu samples after the corrosion test in ~0.1 M NaCl aqueous solution for 0–5 hours. (c) Static water contact angle measurement of the hydrophobic (h-rCu and h-Gr/rCu) copper foils after immersion in ~0.1 M NaCl aqueous solution for 0–5 hours.

(Figure 2c) substrates show additional prominent peaks that correspond to the various oxidation states of copper including CuO, Cu_2O and $Cu(OH)_2$. This indicates that the graphene coating is highly effective as a passivating barrier to suppress oxidation of copper.

We conducted further experiments in electrolyte environments to evaluate the anti-corrosion properties of the graphene coating. We immersed six different samples of h-rCu and h-Gr/rCu in 0.1M NaCl aqueous solution for 5 hours at room temperature. The water contact angle of each sample was measured hourly. We used NaCl in this study since it is the most common chemical found in sea water. **Figures 3**a and b show photographs of water droplets on h-rCu and h-Gr/rCu surfaces for different exposure times to the NaCl solution. Figure 3c shows the averaged (over six samples) static water contact angle measurements carried out using a SEO Phoenix contact angle system (see Experimental Section). As shown in Figure 3c, after one hour, the contact angle of the h-rCu sample was rapidly decreased to ~86°. In fact after five hours, the water contact angle of the h-rCu sample was decreased to ~35° which is lower than the contact angle of bare copper. On the other hand, after 5 hours, the contact angle of h-Gr/rCu sample was maintained at ~125°. These results show the effectiveness of the graphene film as an anti-corrosion barrier with excellent wetting stability. These are important attributes in a variety of applications ranging from thermal management to water harvesting.[22,23] The anti-corrosion properties of the graphene coating was also confirmed by exposing it to various commonly used copper etchants (Figure S7).

To demonstrate the utility of our h-Gr/rCu surface, we performed water harvesting (condensation) experiments via dehumidification using Cu, Gr/Cu, h-rCu and h-Gr/rCu samples. **Figure 4**a depicts the condensation set-up; a thermoelectric cooling module was used to reduce the temperature of the copper surfaces below that of the ambient air and a humidifier and temperature controller were used to control the relative humidity in the chamber. To check for the reproducibility of the results, we tested four separate identical samples of Cu, Gr/Cu, h-rCu and h-Gr/rCu (dimensions of 1 cm × 3 cm) under humid conditions in the test chamber (Figure S8). During the experiment, the temperature and humidity of the chamber, measured by a thermo-hygrometer mounted inside the chamber, was maintained at ~30.0 °C ± 1 and ~80~85%, respectively. The temperature of the four substrates was kept at ~7 ± 0.1 °C, as measured by a thermocouple attached to the thermo-electric cooling module. Droplets condensed on each of the surfaces were drained into containers (placed under each sample) by gravity. Figure 4b shows the comparison of the total mass of water condensed and the dewetting ratio for the various samples tested over a one-hour time period. It is evident that the h-Gr/rCu surface clearly outperforms the Cu, Gr/Cu, and h-rCu surfaces. To understand this behavior we used a high speed camera to record the images of water droplets condensing on the various surfaces (Figures 4c, d, e and f). The Cu and Gr/Cu surfaces show a water contact angle of ~86° and are not hydrophobic enough to enable drop-wise condensation. Instead these surfaces rapidly transition to a film-wise condensation mode as shown in Figures 4c and d. This is also evident in a relatively low de-wetting ratio of ~0.3 (Figure 4b) indicating that the majority of the surface is wet due to the formation of liquid films on the surface. By contrast, the h-rCu and h-Gr/rCu surfaces show dropwise condensation behavior (Figures 4e and f) with higher de-wetting ratios (Figure 4b) due to their significantly higher hydrophobicity (water contact angles >125°). The rate of vapor-to-liquid phase change[11] in such dehumidification experiments is directly related to the heat transfer rate- the higher the heat transfer rate, the more is the quantity of water that can be harvested. It is well established that the liquid films associated with film-wise condensation have higher interfacial thermal resistances[11,23] in comparison to drop-wise condensation which explains the higher heat transfer rate and hence the greater quantities of water condensed by the h-rCu and h-Gr/rCu surfaces compared to Cu and Cu/Gr. It is noteworthy that out of the two surfaces that exhibited dropwise condensation, the h-Gr/rCu surface significantly outperformed the h-rCu

ADVANCED MATERIALS
www.advmat.de

www.MaterialsViews.com

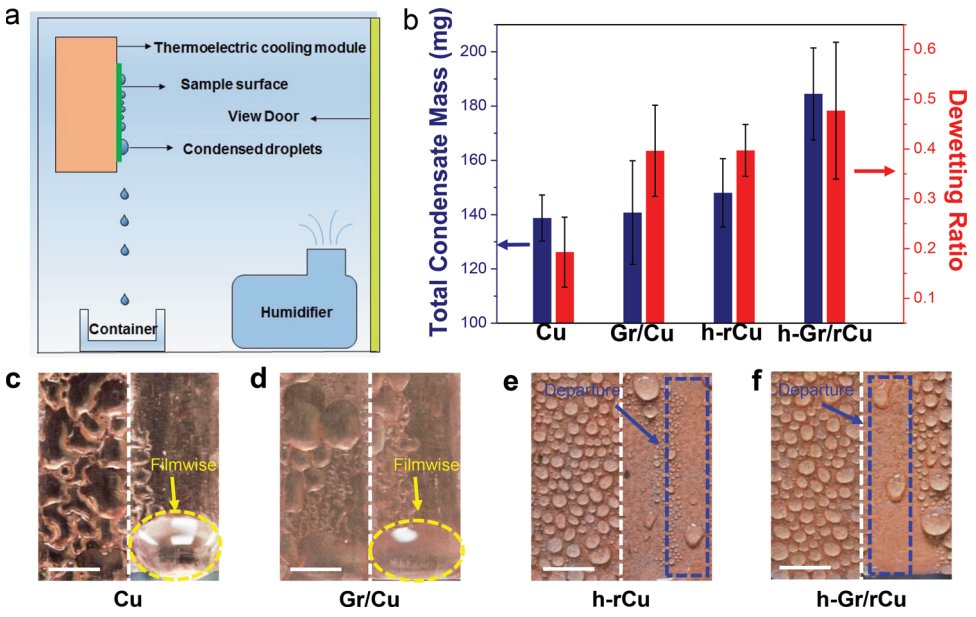

Figure 4. Water harvesting by dehumidification. (a) Schematic diagram of water harvesting test set-up. (b) Total condensate mass and dewetting ratio for the Cu, Gr/Cu, h-rCu and h-Gr/rCu surfaces. (c), (d) Filmwise condensation of water on bare copper (Cu) and graphene coated copper (Gr/Cu), respectively. (e), (f) Dropwise condensation on electroplated and thermal annealed copper with (h-Gr/rCu) and without (h-rCu) graphene coating, respectively. Scale bars in c-f are 5 mm.

surface in terms of its water harvesting capability. This is a result of the superior anti-corrosion and stable wetting properties of the h-Gr/rCu surface vis-à-vis the uncoated h-rCu surface as demonstrated in Figures 2 and 3. Oxidation of the unprotected h-rCu surface will increase the interfacial thermal resistance, while for the h-Gr/rCu surface the wetting-transparent graphene coating provides a thermally-conductive passivation layer that suppresses oxidation while maintaining the inherent hydrophobicity of the underlying surface. One limitation of in-situ growth of the graphene coating by CVD is that this method is limited to metal surfaces such as Copper and Nickel which could limit the maximum achievable water contact angles. However by controlling the surface roughness and hence the porosity (i.e., air-to-solid fraction) of the surface it may be possible to engineer graphene coated super-hydrophobic surfaces, which has important applications in surface science.

To conclude, we have demonstrated for the first time the feasibility of developing 'wetting-transparent' monolayer graphene drapes for strongly hydrophobic (rough) surfaces. They key to this lies in depositing the graphene drape "in situ" by chemical vapor deposition methods so as to ensure that the graphene coating is well-adhered to the surface and follows the contours of the surface. We show that such graphene drapes deliver outstanding anti-corrosion and wetting stability to the underlying surface. Such graphene coated hydrophobic surfaces enable enhanced droplet mobility which is required in a variety of applications. In this study, we have demonstrated one such promising application, namely as a condensation surface for water harvesting.

Experimental Section

Water Contact-angle Measurement: The water contact angle was measured using a SEO Phoenix contact angle system (Surface Electro Optics, Korea) in air environment at room temperature. The volume of the deionized water droplets was ~3 μL which was generated by the automatic dispenser of the contact angle system. By using CCD (charge-coupled device) camera, we took images of the water droplets. For each sample, the water contact angle was measured at three different positions and the average and deviation value was reported.

Electroplating Procedure: 25 μm Cu foil (99.8%) for electroplating and graphene growth was purchased from Alfa Aesar (USA). The Cu foil was electroplated in 0.06 M sulfuric acid and 0.08 M copper sulfate aqueous solution at ambient temperature. The dimensions of the Cu foils used as the anode and cathode in the electroplating cell were 1 × 3 cm and 2 × 3 cm, respectively. The cathode and anode Cu substrates were first sanded to eliminate any surface contamination and the sanded Cu substrates were washed with acetone, ethanol and de-ionized water. The Cu electroplating was performed on a programmable DC power supply (OPS-305, ODA Tech. Korea). The Cu substrate was plated at a constant current density of ~0.08 A/cm^2 for ~10 min. After electroplating, the electroplated Cu foil was dried in a forced convection oven (OF-12, JeioTech, Korea) for ~12 hours.

Micro-Raman Spectroscopy: The Raman spectrum of the h-Gr/rCu and Gr/Cu samples was obtained by using a Dispersive Raman Microscope (ARAMIS, Horiba) equipped with a 514 nm laser and a 50X microscope objective lens.

Graphene Synthesis: The electroplated copper foils were inserted into a quartz tube, and placed in a tube furnace heated to ~850 °C with 17.2 sccm H_2 flow at 160 mtorr. After ~15 min of annealing under these conditions, the temperature was ramped up to ~1000 °C. Then the reaction gas mixture of CH_4 and H_2 were flowed at ~475 mtorr with rates of ~17.2 sccm H_2 and ~51.4 sccm CH_4 for ~10 min. After that, the copper foil was rapidly cooled down to room temperature while flowing ~17.2 sccm H_2 and ~51.4 sccm CH_4 at ~475 mtorr for an hour.

Supporting Information

Supporting Information is available from the Wiley Online Library or from the author.

Adv. Mater. **2014**,
DOI: 10.1002/adma.201401149

Acknowledgements

G. K. and S. G. equally contributed to all experimental results, S. C. contributed to depositing the graphene coating onto the hydrophobic copper surfaces, N. K. developed the fundamental understanding of wetting transparency of graphene-coated surfaces for hydrophobic water-harvesting and I. O. conceived and directed the research project and wrote the paper with N. K.. This work was supported by the Ministry of Trade, Industry and Energy through Technology Innovation Program (Graphene Materials and Components Development Program of MOTIE/KEIT 10044410) and a National Research Foundation of Korea Grant funded by the Korean Government (2012R1A2A2A01047543). N. K. also acknowledges funding support from the John A. Clark and Edward T. Crossan chair professorship at the Rensselaer Polytechnic Institute.

Received: March 13, 2014
Revised: April 10, 2014
Published online:

[1] C. J. Shih, Q. H. Wang, S. C. Lin, K. C. Park, Z. Jin, M. S. Strano, D. Blankschtein, *Phys. Rev. Lett.* **2012**, *109*, 176101.
[2] C. J. Shih, M. S. Strano, D. Blankschtein, *Nat. Mater.* **2013**, *12*, 866.
[3] F. Taherian, V. Marcon, N. F. A. van der Vegt, F. Leroy, *Langmuir* **2013**, *29*, 1457.
[4] Z. Li, Y. Wang, A. Kozbial, G. Shenoy, F. Zhou, R. McGinley, P. Ireland, B. Morganstein, A. Kunkel, S. P. Surwade, L. Li, H. Liu, *Nat. Mater.* **2013**, *12*, 925.
[5] J. Rafiee, X. Mi, H. Gullapalli, A. V. Thomas, F. Yavari, Y. Shi, P. M. Ajayan, N. A. Koratkar, *Nat. Mater.* **2012**, *11*, 217.
[6] F. Mugele, *Nat. Mater.* **2012**, *11*, 182.
[7] L. Zhang, J. Yu, M. Yang, Q. Xie, H. Peng, Z. Liu, *Nat. Commun.* **2013**, *4*, 1443.
[8] E. Singh, A. V. Thomas, R. Mukherjee, X. Mi, F. Houshmand, Y. Peles, Y. Shi, N. Koratkar, *ACS Nano* **2013**, *7*, 3512.
[9] K. Rykaczewski, W. A. Osborn, J. Chinn, M. L. Walker, J. H. J. Scott, W. Jones, C. Hao, S. Yao, Z. Wang, *Soft Matter.* **2012**, *8*, 8786.
[10] C. Li, Z. Wang, P. I. Wang, Y. Peles, N. Koratkar, G. P. Peterson, *Small* **2008**, *4*, 1084.
[11] V. P. Carey, *Liquid-Vapor Phase-Change Phenomena:* An Introduction to the Thermophysics of Vaporization and Condensation Processes in Heat Transfer Equipment, Hemisphere, Washington, D. C, USA, **1992**.
[12] R. Chen, M. C. Lu, V. Srinivasan, Z. Wang, H. H. Cho, A. Majumdar, *Nano Lett.* **2009**, *9*, 548.
[13] X. Liang, B. A. Sperling, I. Calizo, G. Cheng, C. A. Hacker, Q. Zhang, Y. Obeng, K. Yan, H. Peng, Q. Li, X. Zhu, H. Yuan, A. R. Hight Walker, Z. Liu, L. M. Peng, C. A. Richter, *ACS Nano* **2011**, *5*, 9144.
[14] X. Li, W. Cai, J. An, S. Kim, J. Nah, D. Yang, R. Piner, A. Velamakanni, I. Jung, E. Tutuc, S. K. Banerjee, L. Colombo, R. S. Ruoff, *Science* **2009**, *324*, 1312.
[15] K. S. Kim, Y. Zhao, H. Jang, S. Y. Lee, J. M. Kim, K. S. Kim, J. H. Ahn, P. Kim, J. Y. Choi, B. H. Hong, *Nature* **2009**, *457*, 706.
[16] P. Dhiman, F. Yavari, X. Mi, H. Gullapalli, Y. Shi, P. M. Ajayan, N. Koratkar, *Nano Lett.* **2011**, *11*, 3123.
[17] R. N. Wenzel, *Ind. Eng. Chem.* **1936**, *28*, 988.
[18] J. Rafiee, M. A. Rafiee, Z. Z. Yu, N. Koratkar, *Adv. Mater.* **2010**, *22*, 2151.
[19] A. B. D. Cassie, S. Baxter, *Trans. Faraday Soc.* **1944**, *40*, 546.
[20] S. Chen, L. Brown, M. Levendorf, W. Cai, S. Y. Ju, J. Edgeworth, X. Li, C. W. Magnuson, A. Velamakanni, R. D. Piner, J. Kang, J. Park, R. S. Ruoff, *ACS Nano* **2011**, *5*, 1321.
[21] D. Prasai, J. C. Tuberquia, R. R. Harl, G. K. Jennings, K. I. Bolotin, *ACS Nano* **2012**, *6*, 1102.
[22] X. Chen, J. Wu, R. Ma, M. Hua, N. Koratkar, S. Yao, Z. Wang, *Adv. Funct. Mater.* **2011**, *21*, 4617.
[23] C. Graham, P. Griffith, *Int. J. Heat Mass Transfer* **1973**, *16*, 337.